

***Centella Asiatica* Extract Containing Bilayered Electrospun Wound Dressing**

Ismail Alper Isoglu* and Nuray Koc

Department of Bioengineering, Abdullah Gül University, Kocasinan, Kayseri 38080, Turkey

(Received September 3, 2019; Revised October 31, 2019; Accepted November 5, 2019)

Abstract: Innovative and bioactive wound dressings prepared by electrospinning mimicking the native structure of the extracellular matrix (ECM) have gained significant interest as an alternative to conventional wound care applications. In this study, bilayered wound dressing material was produced by sequential electrospinning of quaternized poly(4-vinyl pyridine) (upper layer) on the *Centella Asiatica* (CA) extract containing electrospun poly(D, L-lactide-co-glycolide) (PLGA)/poly(3-hydroxybutyrate-co-3-hydroxy valerate) (PHBV) blend membrane (lower layer). Scanning electron microscopy (SEM) was utilized to show a uniform and bead-free fiber structure of electrospun membranes. The average diameter of CA extract containing electrospun PLGA/PHBV blend membrane was calculated $0.471\pm 0.11\ \mu\text{m}$, whereas the average fiber diameter of electrospun poly(Q-VP) membranes was in the range of $0.460\pm 0.057\ \mu\text{m}$. Chemical, thermal, mechanical properties, and adsorption capacity of electrospun membranes, as well as the cumulative release of CA from the electrospun PLGA/PHBV membrane, were investigated. Viability, adhesion, and attachment of human fibroblast cells on the electrospun membranes on pre-set days were evaluated by the colorimetric CellTiter 96[®] Aqueous One Solution Cell Proliferation Assay (MTS assay) and SEM. Results revealed that CA loaded bilayered electrospun wound dressing showed promoted attachment and proliferation of fibroblasts. Hence, it can be concluded that CA extract containing bilayered electrospun wound dressing prepared in this study has a promising potential for wound healing applications.

Keywords: Wound dressing, Electrospinning, Bilayered, *Centella Asiatica*

Introduction

Skin, the largest organ of the body with self-healing ability, plays a crucial role in many activities, including acting as a barrier against pathogen attacks, protecting the underlying organs from external damages, and providing fluid and gas homeostasis [1,2]. Different types of factors, such as wounds, burns, and injuries, can easily damage skin tissue [3]. The treatment of large-scale skin defects remains still a substantial clinical problem, which negatively affects the life quality of millions of people around the world [4].

Wound healing is an interactive process possessing several complicated phases, including inflammation, granulation, and re-epithelialization (new tissue formation), contraction, and regeneration of tissues [5-7]. Conventional skin substitutes such as autografts, allografts, and xenografts have not provided an effective treatment of skin tissue lost due to their drawbacks such as the limitation of donor sites, enzymatic resistance, reduced longevity, and antigenicity [8]. Thus, in recent years, scientists have focused on the novel therapeutic wound dressing materials with a capacity to accelerating wound healing and preventing bacterial growth together [9,10].

Electrospinning is a well-known and versatile technique to fabricate porous membranes possessing fibers with an average diameter in size ranging from nanometers to micrometers, which make them great candidates for wound healing applications [11,12]. Due to their unique structure mimicking the natural extracellular matrix (ECM) morphologically, electrospun membranes provide large surface-

area-to-volume and gas permeability, which promote cell migration and adhesion on the wound area, moisture retention, and highly efficient exudate absorption [13,14]. Various natural polymers such as collagen, fibrinogen, chitin, chitosan, some glycosaminoglycans, starch, dextran, alginate and microbial polyesters (polyhydroxyalkanoates (PHA)) and biocompatible synthetic polymers including poly(α -hydroxy acids), poly(ϵ -caprolactone), poly(α -amino acids), poly(orthoesters), poly(anhydrides), poly(alkyl-2-cyanoacrylates) and poly(phosphazenes) can be utilized for preparing electrospun membranes as potential wound healing materials [15]. Among the poly(α -hydroxy acids), poly(D, L-lactide-co-glycolide) (PLGA), FDA approved biocompatible copolymer, has been widely used in wound healing applications, due to its unique properties such as easily electro spinnability, minimal inflammatory response and adjustable degradation time *in vivo* and *in vitro* [16-18]. Poly(3-hydroxybutyrate-co-3-hydroxy valerate) (PHBV) is a member of polyhydroxyalkanoates (PHA) and serves significant to healthcare society as wound healing material [19,20]. However, both these polymers have some drawbacks individually in terms of hydrophobicity and mechanical durability. In order to overcome these problems, electrospun membranes prepared from various blends of both PLGA [21-23] and PHBV [24-26] with natural and synthetic polymers have been investigated as wound dressings.

One of the essential characteristics of an ideal wound dressing is acting as a barrier against the microbial attacks and protects the wound area from infection [27]. To do so, some antibacterial and antimicrobial agents, as well as natural medical plant extracts, have been incorporated into electrospun membranes in order to prevent wound infection,

*Corresponding author: alper.isoglu@agu.edu.tr

accelerate the healing process and reduce scar formation [28,29].

Centella Asiatica (CA), a medicinal plant, has been used in traditional medicine in many parts of the world, including Asia and the Middle East countries to treat small-scale wound areas, hypertrophic scars and damaged skin tissue caused by burns [30-32]. The main pharmacologically active components of CA are saponin-containing triterpene acids and their sugar esters, of which Asiatic acid, asiaticoside, and madecassic acid are considered to be the most effective [33,34]. Among these components, asiaticoside is the primary therapeutic substance and accelerates the wound healing process and reduces scar formation, while asiaticoside provides fibroblast proliferation and ECM synthesis in the wound area. It was also reported that madecassoside effects significantly on wound healing in terms of antioxidant activity, collagen synthesis, and angiogenesis [11,35]. Kosalwatna *et al.* reported that the cream containing 1 % CA extract cream exhibits significant wound healing of chronic ulcer in width, length, and depth after 21 days of usage [36]. Shukla *et al.* investigated the topical application of asiaticoside in regular as well as in diabetic animals and demonstrated a significant enhancement wound healing activity as assessed by an increase in collagen synthesis and tensile strength of the wound tissues [37]. In another study conducted by Maqugart *et al.*, triterpenes from CA were shown to increase the remodeling of the collagen matrix and stimulate glycosaminoglycan synthesis in a rat model [38]. Liu *et al.* approved antioxidative activity, collagen synthesis, and angiogenesis properties of the madecassoside isolated from CA for burn wound healing in mice model [39]. In another study published in 2016 by Zhang *et al.*, it was developed a porous microsphere for the topical delivery of asiaticoside to increase its absorption and improve its therapeutic effects, as well as to supply a novel preparation with potential for clinical wound treatment [40]. Sikarepaisan *et al.* investigated the potential of electrospun gelatin fiber mats as carriers for topical delivery of a methanolic crude extract of CA and the release characteristic of asiaticoside from the CA-loaded gelatin fiber mats [41]. In a similar study belong to Yao *et al.*, it was investigated the potential of electrospun gelatin membranes containing CA extract as topical/transdermal wound dressings [42]. Based on the previous studies that showed the significant healing and scar reducing effects of CA on the different types of wounds, including traumatic, surgical, diabetic, and burn, in the present study, we chose the extract of CA to obtain active and innovative wound dressing material.

On the other hand, the polymers containing quaternary ammonium salts have widely studied to fabricate antimicrobial wound dressings with no toxic effect. Chemically modified poly(4-vinyl pyridine) (poly(4-VP)) is one of these polymers and has been investigated in the literature as wound healing material [43].

In this study, we aimed to fabricate and characterize a bilayered fibrous wound dressing prepared by electrospinning technique, which consists of CA extract containing electrospun PLGA/PHBV membrane as lower layer contacting directly the wound surface and electrospun quaternized poly(4-VP) as upper layer protecting the wound area from microbial attacks. We also investigated the viability, adhesion, and attachment of human fibroblast cells on the wound dressing.

Experimental

Materials

Poly(D,L-lactide-co-glycolide) (PLGA, DL-Lactide:Glycolide copolymer, ratio M/M%: 75/25, MW=120,000; CAS No.26780-50-7) was purchased from Purac Biomaterials. Poly(3-hydroxybutyrate-co-3-hydroxy valerate) (PHBV, natural origin, PHV content 12 mol%, Mn=280,000, Mw=690,000; CAS No.80181-31-3) was purchased from Aldrich Co. (USA). 4-Vinylpyridine (CAS No.100-43-6) was purchased from Aldrich. *Centella Asiatica* (CA, natural extract in powder form, CAS No.16830-15-2) was obtained from Wuhan Yuancheng Technology Development Co. Ltd. (China). 6-Bromo caproic acid (%97, CAS No. 4224-70-8) was purchased from Aldrich. 2,2'-Azobis(2-methylpropionitrile) (AIBN, CAS No.78-67-1) was purchased from Aldrich. Human fibroblast cells were kindly donated by Erciyes University Genom and Stem Cell Center, Kayseri. All other chemicals and solvents are used without further purification.

Fabrication of CA Containing Bilayered Wound Dressing

Bilayered wound dressing was fabricated by sequential and continuous electrospinning of quaternized poly(4-vinyl pyridine) (upper layer) on the CA containing electrospun PLGA/PHBV blend membranes (lower layer). All electrospinning experiments were conducted at room temperature, and all membranes were vacuum dried overnight, stored in dry cabinets, and used for further studies. The fabrication process was conducted in two stages:

Preparation of Lower Layer (CA Loaded PLGA/PHBV Electrospun Membranes)

We first optimized the concentrations of PLGA/PHBV blend solutions and determined the type of solvent/solvent mixture for electrospinning in order to obtain electrospun membranes possessing a bead-free structure and uniform fibers with minimum average diameter. The other electrospinning parameters, such as applied voltage, flow rate, and the distance between the tip and the collector, were kept constant. To do so, we prepared PLGA/PHBV blend solutions at the ratio of 75:25 (w/w) with different concentrations (5, 10, 20 %, w/v). Chloroform (CHCl₃), 1,1,1,3,3,3-hexafluoro-2-propanol (HFIP) and their mixture were used in different ratios (50:50, 75:25 v/v) as the solvent. Each blend solution was magnetically stirred at room temperature for 3 h, filled into a 10 ml syringe with

21G needle (with an inner diameter of 14.53 mm), and then placed on a syringe pump (NE-1000 Syringe Pump, New Era Pump Systems, USA). The electrospinning parameters were set as 20 kV of high voltages (NE100, Inovenso, Turkey), 1.5 ml/h of the flow rate, and 15 cm of the distance between the tip and the collector.

Centella Asiatica Loading

Based on the results above, the PLGA/PHBV blend (75:25 w/w) solution prepared in pure HFIP was used for CA loading experiments. Briefly, PLGA and PHBV pellets were dissolved in HFIP at the ratio of 75:25 (w/w) and CA extract were added to the PLGA/PHBV blend solution at different ratios (1, 5 and 10 %, w/v) with the final concentration of 20 % w/v. The electrospinning parameters mentioned above were applied (the voltage: 20 kV, the flow rate: 1.5 ml/h, and the distance between the tip and the collector: 15 cm).

Preparation of Upper Layer (Electrospun Poly(Q4-VP) Membrane)

Synthesis and Quaternization of Poly(4-VP)

Electrospun quaternized poly(4-VP) membrane that we designed in our previous study was used as the upper layer of the wound dressing [43]. In the mentioned study, we applied 4 and 8 days of quaternization process and achieved antimicrobial characteristics with 8-days of quaternization. Therefore, we applied the same procedure in our current study to obtain an antimicrobial polymer. Briefly, we first synthesized poly(4-VP) from the 4-vinyl pyridine monomer by free radical polymerization. The AIBN was used as the initiator, and DMF used as the solvent. We kept the monomer/initiator ratio at 500:1 and purged the mixture with nitrogen for 30 min before polymerization. The reaction occurred at 65 °C for 20 h. Afterward, the product was purified by precipitation from toluene three times and stored in a vacuum oven for the quaternization step. For quaternization, synthesized poly(4-VP) was reacted with 6-bromocaproic acid as a quaternization agent at the ratio of 1:2 (v/v) in methanol, and the mixture was purged with nitrogen gas for 30 min. The solution was refluxed in the oil bath at 65 °C at 450 rpm for eight days. The quaternized polymer (poly(Q4-VP)) was successfully obtained after the product was purified by precipitation from diethyl ether [43]. Quaternization, which can be accepted as a confirmation for the antimicrobial characteristic based on our previous study, was confirmed by FT-IR analysis. Note that we did not repeat the antimicrobial test here, as we already reported it in İsoğlu *et al.* [43].

Electrospinning of Poly(Q4-VP)

The quaternized poly(Q4-VP) were dissolved in DMF for preparing electrospinning solutions at different concentrations (40, 50, 60, 70 % w/v). Each solution was fed into a 10 ml syringe with a 21G needle (with an inner diameter of 14.53 mm) and seated on a motorized and programmable syringe pump (NE-1000 Syringe Pump, New Era Pump Systems, USA). The electrospinning process parameters were set as follows: the applied voltage was in the range of

18 kV, the distance between the tip and the collector was 15 cm, and the flow rate was 1 ml/h.

Characterization

Morphological Study

Scanning electron microscopy (SEM) (Carl Zeiss EVO LS10, Germany) was utilized to indicate the morphology of all electrospun membranes. The Image J software (National Institutes of Health, Bethesda, MD) was used to calculate the average fiber diameters from SEM images.

Fourier Transform Infrared (FT-IR) Analysis

The FT-IR spectra of the electrospun membranes and neat CA extract were recorded by using Nicolet 6700 FT-IR Spectrometer (Thermo Scientific, USA) in the range of 400-4000 cm^{-1} .

Thermal Analysis

Thermal properties of electrospun membranes were determined by differential scanning calorimetry (DSC) (Perkin Elmer, USA) at a heating rate of 2 °C min^{-1} from 0 to 200 °C.

Absorption of Wound Fluid

In order to mimic wound fluid, Pseudo Extra Cellular Fluid (PECF) was used, which was prepared by dissolving sodium chloride (NaCl), potassium chloride (KCl), sodium hydrogen carbonate (NaHCO_3) and hydrogen phosphate (K_2HPO_4) in distilled water at a pH value of 8 [46]. The 1×1.5 cm rectangular samples of electrospun PLGA/PHBV (75:25 w/w, %20 w/v) membranes with CA (1 % w/w) and without CA, PLGA/PHBV (75:25 w/w, %20 w/v) film prepared by solvent casting method in Petri dishes were first weighed and placed into the 24-well plate filled with PECF, which were kept in an incubator at 37 °C for 24 h. The samples were weighed after the excess of the solution was removed by blotting with filter paper. The percentage of absorption capacity of membranes was calculated as follows:

$$\text{Absorption ratio (\%)} = (W_s - W_0)/W_0 \times 100 \quad (1)$$

where W_0 is the weight of the initial dry sample and W_s is the weight of the swollen sample.

Mechanical Analysis

The evaluation of tensile strengths and elongation at the break of electrospun membranes was performed by using Autograph AGS-X 10 kN (Shimadzu, Japan) device. The samples were cut into the strips with 60 mm in length, 20 mm in width possessing a thickness of 0.1 mm. Tensile tests were conducted at the strain rates of $1 \times 10^{-1} \text{ s}^{-1}$ at room temperature.

In vitro Drug Release Study

Asiaticoside absorbance was monitored to determine the *in vitro* release profile of the CA from the PLGA/PHBV electrospun membrane at 215 nm. First, the calibration curve of the asiaticoside solution was plotted with 0.5, 0.1, 0.05, 0.01, 0.001 mg/ml in water. PLGA/PHBV (75:25 w/w, %20

w/v) electrospun membrane with CA (1 % w/w) was placed into a 10 ml PBS solution, and a determined time interval 1 ml sample solution was withdrawn, and a new PBS solution was added to this medium. The absorbance of the withdrawn sample was measured at 215 nm. The cumulative release of CA was calculated using the following equation;

$$\begin{aligned} & \text{Cumulative percentage release (\%)} \\ &= \frac{\text{Volume of sample withdrawn (ml)} \times P(t-1)}{\text{Bath volume (v)} + Pt \text{ release}} \quad (2) \end{aligned}$$

where Pt is percentage release at time t and $P(t-1)$ is percentage release previous to t .

Assessment of Cell Viability

As dermal fibroblasts have a crucial contribution to the wound healing process, we used human fibroblast cells for assessment of the biocompatibility of the electrospun membranes. Human fibroblasts were cultured with 10 ml Dulbecco's minimum essential medium (DMEM, Gibco® Life Technologies, Darmstadt, Germany) with supplements of 4.5 mg m^{-1} glucose, 10 % fetal bovine serum and 1 % penicillin and streptomycin in 10 cm^2 tissue culture flasks. The cells were kept in an incubator at 37 °C with 5 % CO_2 . The viability of the cells on the membranes was determined by using the MTS assay (CellTiter 96®, Promega, Madison, Wisconsin, USA). Electrospun PLGA/PHBV (75:25 w/w, 20 % w/v) membranes with (1 % w/v) and without CA and electrospun poly(Q-4VP) were cut into the rectangular shape (5×2.5 mm). The samples were soaked in ethanol solution (70 % v/v) for 2 h and kept under UV for 1 h [27,44]. Afterward, the cells were seeded on the samples placed in 96-well plates (1×10^4 cells/well). The cells/membrane

structures were incubated at 37 °C in a humidified incubator of %5 CO_2 for pre-set days. After 1, 3, and 7 days of culture, the electrospun membrane samples were incubated in 20 μ l of MTS reagent at 37 °C for 4 h. Subsequently, the absorbance of the medium was measured at 490 nm using a 96-well plate reader (Varioskan Lux, Thermo Scientific, USA) [45].

Assessment of Cell Proliferation and Attachment

SEM was used for the assessment of cell proliferation and attachment on the electrospun membranes. The cells/membrane structures were prepared, as described in the previous paragraph. After pre-set days (1, 4, and 7 days), the samples were rinsed three times with PBS buffer to remove non-adherent cells and immobilized with glutaraldehyde solution (2.5 % (v/v)) at 4 °C for 2 h. Then, each sample was dehydrated through a series of gradient ethanol solutions of 30 %, 50 %, 70 %, 90 %, and 100 % for ten minutes and air-dried for SEM evaluation [46].

Results and Discussion

Fabrication of CA Loaded Bilayered Electrospun Wound Dressing

Lower Layer

It is well known from the literature that the electrospun membranes prepared from blends of synthetic and natural polymers have several advantages comparing to individual polymers [47]. Based on this fact, we produced the electrospun membrane made of PLGA/PHBV blend containing CA to prepare the lower layer of the bilayered wound dressing. We first conducted preliminary electrospinning

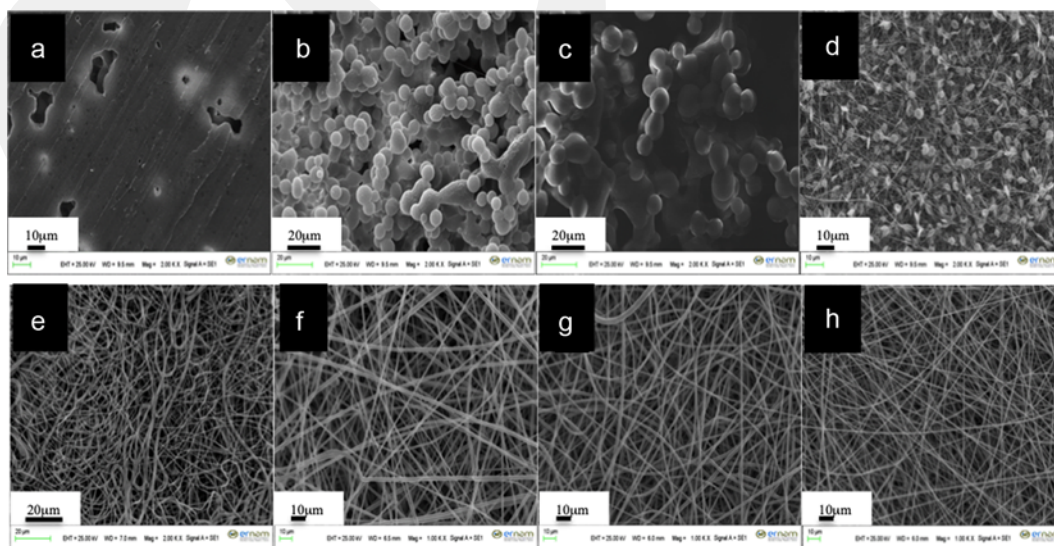


Figure 1. SEM images of electrospun PLGA/PHBV (75:25, w/w) membranes as a function of concentrations and type of solvent/solvent mixture; (a) 5 %, in pure $CHCl_3$, (b) 5 %, in HFIP/ $CHCl_3$ mixture (50:50, v/v), (c) 10 %, in pure $CHCl_3$, (d) 10 %, in HFIP/ $CHCl_3$ mixture (50:50, v/v), (e) 20 %, in pure $CHCl_3$, (f) 20 %, in HFIP/ $CHCl_3$ mixture (50:50, v/v), (g) 20 %, in HFIP/ $CHCl_3$ mixture (75:25, v/v), and (h) 20 %, in pure HFIP.

experiments to adjust concentrations of PLGA/PHBV blend solutions and the type of solvent/solvent mixture. The other electrospinning parameters, such as applied voltage, flow rate, and the distance between tip and collector, were kept constant. SEM images of the membranes possessing bead-free structure and continuous fibers with homogenous diameter distribution were used for the optimization of process parameters.

Figure 1 shows SEM images of electrospun membranes prepared from different solvents at different concentrations. As seen from Figure 1, no fibers were formed at 5% polymer concentration independent of solvent, while many beads formation was observed at 10% polymer concentration (Figure 1(a-d)). However, electrospun PLGA/PHBV (75:25, w/w) membranes, which possess appropriate bead-free structure and homogeneously distributed fibers, were

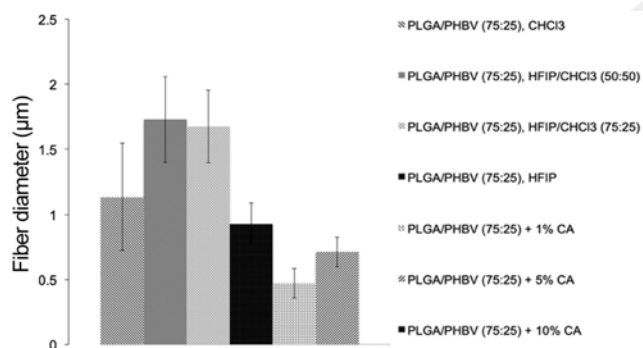


Figure 2. Average fiber diameter of electrospun PLGA/PHBV (75:25, w/w) membranes with and without CA. Error bars represent \pm SD.

obtained from polymer solutions prepared from pure HFIP and HFIP/CHCl₃ mixture at 20% concentration (Figure 1(f-h)). As mentioned before, the operating parameters were set 20 kV of the applied voltage and 1.5 ml/h of flow rate and 15 cm of distance between tip and collector. Image J software was used to calculate the mean of fiber diameters by measuring the diameters of randomly selected 50 fibers in the SEM images. The average fiber diameter of electrospun PLGA/PHBV (75:25, w/w) blend membranes prepared with solvent mixture were calculated $1.314 \pm 0.44 \mu\text{m}$ (in pure CHCl₃), $1.728 \pm 0.33 \mu\text{m}$ (in HFIP/CHCl₃ mixture, 50:50, v/v), $1.673 \pm 0.28 \mu\text{m}$ (in HFIP/CHCl₃ mixture, 75:25, v/v) and $0.929 \pm 0.13 \mu\text{m}$ (in pure HFIP), respectively (Figure 2).

Among these electrospun membranes, we selected PLGA/PHBV (75:25, w/w) blend membrane dissolved in pure HFIP for CA loading experiments, since its fibers oriented more homogeneously with narrower diameter distribution. Besides, HFIP is a commonly used organic solvent, which is known from the literature that it can be entirely evaporated after the electrospinning process without leaving any residue on the fibers [48]. Different amounts of CA extract (1% and 5%, 10% w/v) were added to PLGA/PHBV (75:25, w/w) solution prepared from pure HFIP, and the polymer solutions with CA extract were electrospun under the conditions as mentioned earlier. Figure 3 shows representative SEM images of PLGA/PHBV electrospun membranes containing different amounts of CA extract. The average diameter of CA loaded PLGA/PHBV membranes were calculated $0.471 \pm 0.11 \mu\text{m}$ for PLGA/PHBV membrane with 1% CA amount and $0.714 \pm 0.11 \mu\text{m}$ for PLGA/PHBV membrane with 5% CA amount via Image J software (Figure 2).

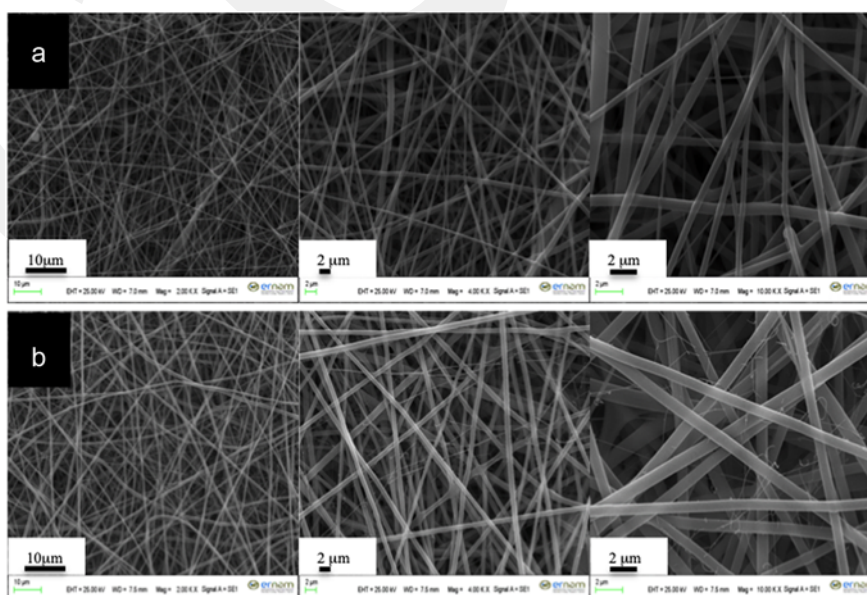


Figure 3. SEM images of electrospun PLGA/PHBV (75:25, w/w) membrane containing CA extract; (a) 1% (w/v) and (b) 5% (w/v).

According to the SEM images, we observed that the fiber diameters were decreased after adding CA to the polymer solutions, which complies with the results of the previous studies [49]. As the ratio of CA increased to 5 %, some deformations on fibers were observed, and the diameter distribution became wider comparing to the neat membrane. When we increased the CA ratio to 10 %, the viscosity of the PLGA/PHBV blend solution became very low. Thus, the PLGA/PHBV blend solution containing 10 % CA extract

was not appropriate for electrospinning. Membranes electrospun from a polymer solution with an insufficient viscosity may become unstable and exhibit an inconsistent morphology [42]. According to SEM images of CA loaded PLGA/PHBV membranes, we eventually decided to use the electrospun PLGA/PHBV (75:25, w/w, 20 % w/v) membrane having 1 % of CA (w/v) with final concentration of 20 % (w/v) extract as lower layer of the wound dressing material because of its appropriate fiber morphology. Hereafter, in

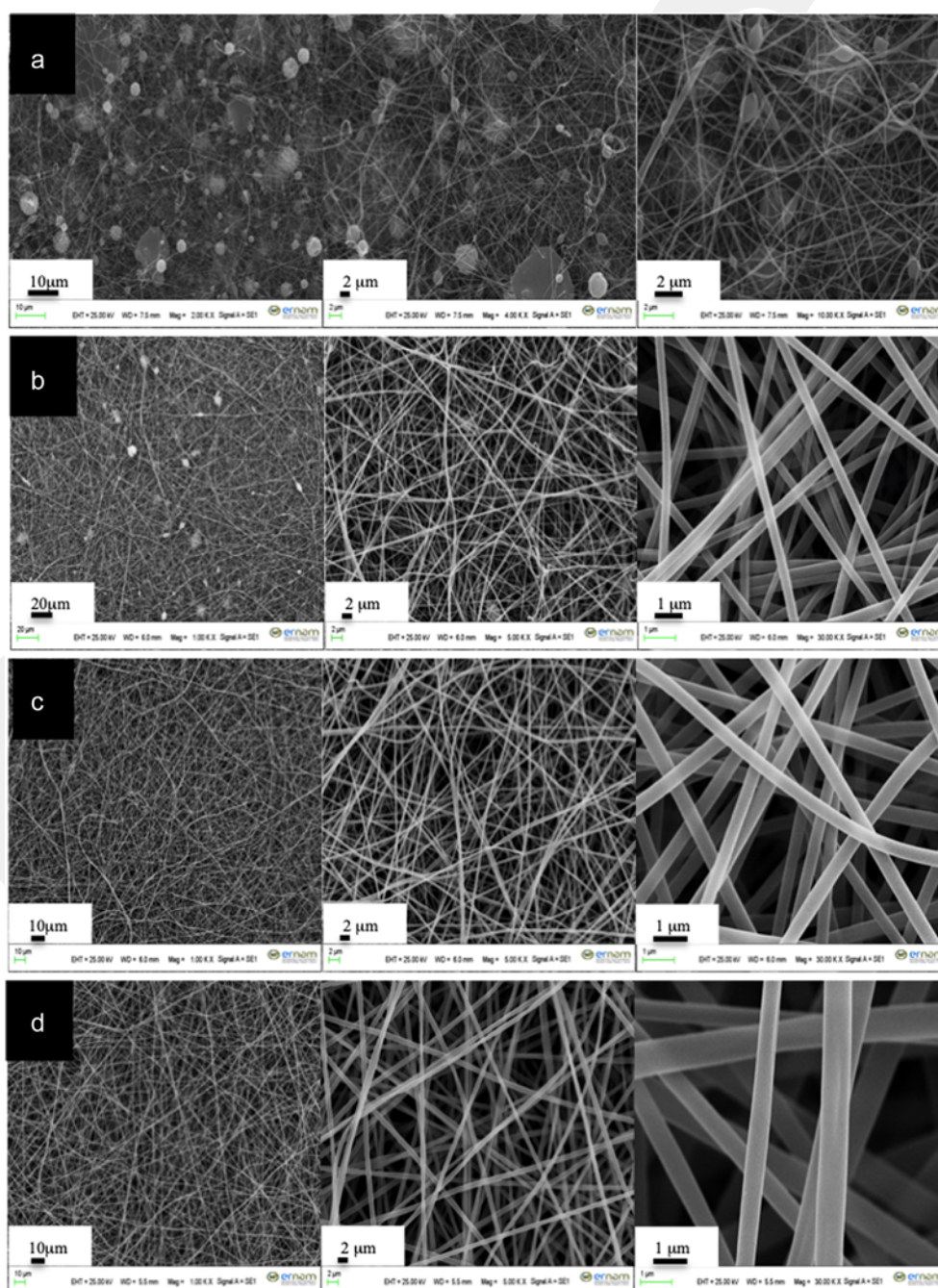


Figure 4. SEM images of poly(Q-4VP) at varying concentrations; (a) 40 %, (b) 50 %, (c) 60 %, and (d) 70 %.

this manuscript, the electrospun PLGA/PHBV (75:25, w/w, 20 % w/v) membrane containing 1 % of CA (w/v) with the final concentration of 20 % (w/v) will be represented as electrospun PLGA/PHBV membrane with CA.

Upper Layer

The upper layer of the bilayered wound dressing was prepared from electrospun quaternized poly(4-vinyl pyridine) that we designed in our previous study [43] since it possesses nanofibrous structure and natural antibacterial characteristics because of quaternary ammonium groups through the polymer chain. Before electrospinning, we first synthesized poly(4-VP) and conducted 8 days-long quaternization process, which was confirmed via FT-IR spectrum and discussed detailed in the structural analysis part of the manuscript below.

After characterization, poly(Q-4VP) solutions were prepared at different concentrations (40, 50, 60 and 70 w/v) in DMF and electrospun with operating conditions of 18 kV and 1 ml/h of flow rate with a fixed tip-collector distance of 15 cm. Figure 4 represents SEM images of electrospun poly(4-VP) membranes at different concentrations. It can be seen that some bead formation was observed at 40 % and 50 % concentrations, while uniform and smooth nanofibers with very narrower diameter distribution were obtained at 60 % and 70 % concentrations. Image J software was also used for calculating the average diameters of fiber by

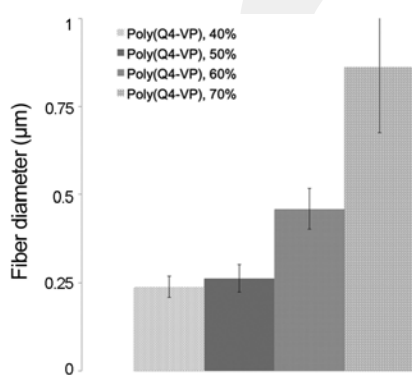


Figure 5. The average fiber diameter of electrospun poly(Q4-VP) membranes at different concentrations. Error bars represent \pm SD.

measuring the diameters of randomly selected 50 fibers in the SEM images. The average fiber diameter of electrospun poly(Q-VP) membranes were calculated as $0.239 \pm 0.03 \mu\text{m}$ (at 40 % concentration), $0.263 \pm 0.04 \mu\text{m}$ (at 50 % concentration), $0.460 \pm 0.057 \mu\text{m}$ (at 60 % concentration) and $0.862 \pm 0.187 \mu\text{m}$ (at 70 % concentration), respectively (Figure 5).

Among resulting membranes, we selected electrospun poly(Q-4VP) with the concentration of 60 % as the upper layer of bilayered electrospun mat, since it possesses uniform nanofiber morphology with narrower diameter distribution. Hereafter, in this manuscript, the electrospun eight days long quaternized poly(4-VP) with a final concentration of 60 % (w/v) will be represented as poly(Q-4V). Eventually, we obtained CA containing bilayered electrospun wound dressing (Figure 6).

FT-IR Analysis

Lower Layer

FT-IR spectra of pure PLGA, PHBV, electrospun PLGA/PHBV membrane, CA loaded electrospun PLGA/PHBV membrane and, neat CA extract are shown in Figure 7. From the spectrum of PLGA samples, it can be seen that an active C=O stretching band at 1750 cm^{-1} existed [50]. PLGA showed several characteristic peaks at 2990 and 2940 cm^{-1} , 1183 , and 1083 cm^{-1} that were assigned to $-\text{CH}_3$, and C-O stretching, respectively [51]. In the spectrum of PHBV, the absorption of the saturated ester C=O groups appeared at 1720 cm^{-1} . The absorption peak at 1276 cm^{-1} in the FT-IR spectrum of PHBV indicates the strong C-O stretching band, which further confirms the presence of the ester functional group [19]. All the characteristic peaks belong to PLGA and PHBV appeared both in the spectra of electrospun PLGA/PHBV and CA loaded electrospun PLGA/PHBV membranes. These FT-IR spectra confirmed that both PLGA and PHBV integrated with the structure and electrospinning did not cause any change in the chemical structure of the blend membrane.

In the FT-IR spectrum of neat CA, the peak at 3271 cm^{-1} indicates the presence of carboxylic acid with O-H stretching vibrations, while the peaks at 2926 , 1645 , 1452

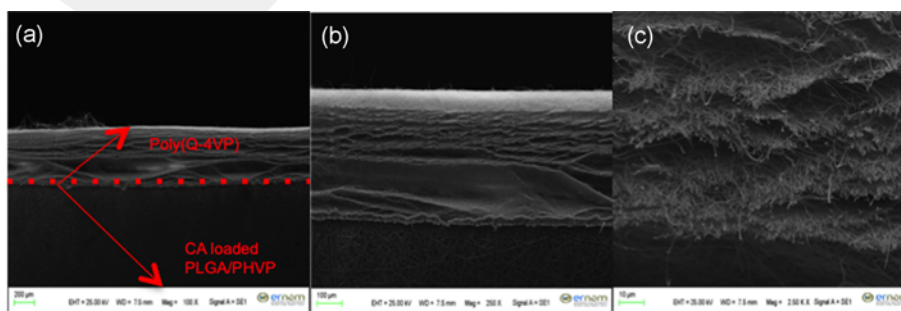


Figure 6. SEM images of CA containing bilayered electrospun membrane with electrospun poly(Q4-VP) upper layer and CA loaded electrospun PLGA/PHBV lower layer; (a) 100 \times , (b) 250 \times , and (c) 2500 \times .

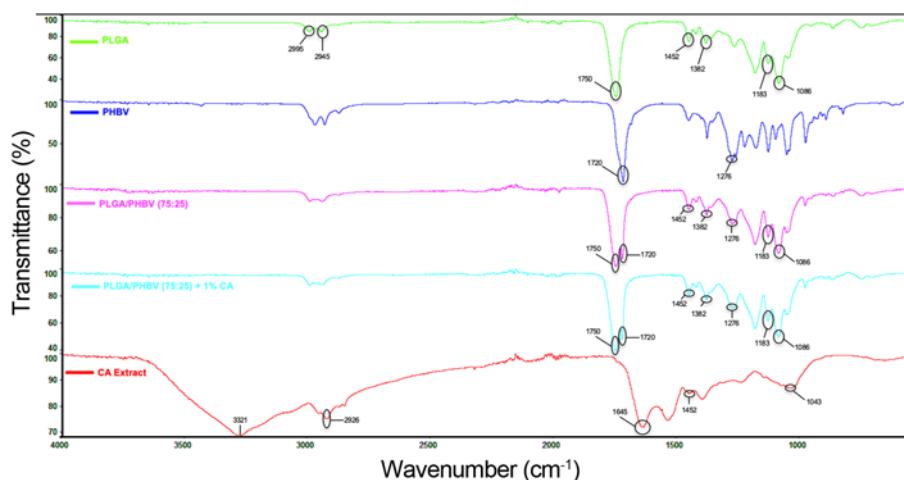


Figure 7. FT-IR spectra of PLGA, PHBV, electrospun PLGA/PHBV membrane, electrospun PLGA/PHBV membrane with CA and neat CA extract.

and 1043 cm^{-1} indicate the presence of alkyl groups, alkenes, alkyl halides, and chloroalkanes in the extract of CA, which were shown to be similar to the previous studies [52,53]. As a meager amount of asiaticoside was added into the electrospun membrane, the peaks belong to CA extract did not appear in the spectrum of CA extract containing PLGA/PHBV electrospun membrane. The FT-IR results coincide well with the previous studies in the literature.

Upper Layer

The upper layer of the bilayered wound dressing was prepared from electrospun quaternized poly(4-vinyl pyridine). To do so, we first synthesized poly(4-VP) by random radical polymerization of 4-VP and characterized by the FT-IR analysis (Figure 8). According to the spectrum, the characteristic peaks of poly(4-VP) at 3057 , 1670 , 1450 , and 1165 cm^{-1} may be assigned to aromatic C-H stretching, aromatic C=C stretching, and C-N stretching [54]. The comparison of the spectrum of poly(4-VP) to the spectrum of poly(Q4-VP), the new peaks appeared at 1640 and

1720 cm^{-1} , which may be assigned to quaternary ammonium and carboxylic acid groups (from caproic acid), respectively [55]. The peak at 3400 cm^{-1} also supported that caproic acid was associated with polymer structure resulting quaternization of the pyridine unit. We calculated the quaternization degree as 45 % by using absorbance values of the peaks for poly(4-VP) and quaternary form (1670 and 1720 cm^{-1}) according to the method given in literature [43]. Thus, the FT-IR spectra confirm the quaternization of poly(4-VP), which is a kind of approval of antimicrobial property as we have already tested by our group before. In our previous study, we applied eight days of the quaternization process and achieved antimicrobial characteristics. In this study, as we used the same quaternary polymer, we applied the same procedure to obtain quaternized polymer with determined antimicrobial characteristics [43].

Thermal Analysis

The thermal properties of pure PLGA, PHBV, and electrospun PLGA/PHBV membrane were investigated by using DSC (Figure 9). According to the DSC thermograms, the amorphous nature of PLGA as it only shows the glass transition temperature (T_g) $47.86\text{ }^\circ\text{C}$. The standard double melting temperatures of pure PHBV were observed at 144.17 and $155.39\text{ }^\circ\text{C}$ due to the formation of various crystals and their melting, recrystallization, and remelting, which was previously reported in the literature [56,57]. For electrospun PLGA/PHBV blend membrane, double melting peaks were also appeared at 145.66 and $155.43\text{ }^\circ\text{C}$, while single peak attributed to T_g of PLGA was seen at $46.09\text{ }^\circ\text{C}$, which is a bit lower than that T_g of PLGA due to improvement in the orientation of molecular chains in the electrospun and as well as the larger area to volume ratio of electrospun fibers [58]. These results indicated the miscibility of pure PLGA and PHBV in the electrospun PLGA/PHBV

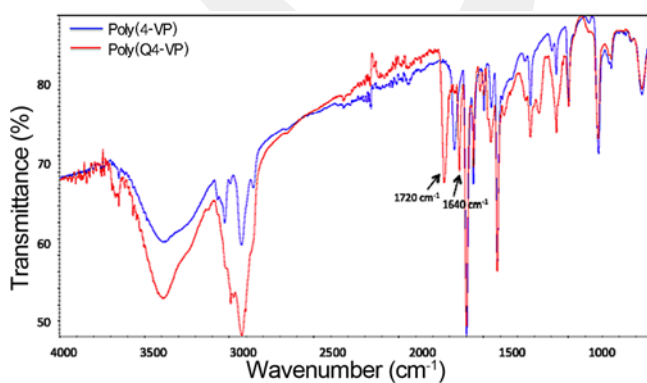


Figure 8. FT-IR spectra of neat poly(4-VP) and quaternized poly(4-VP).

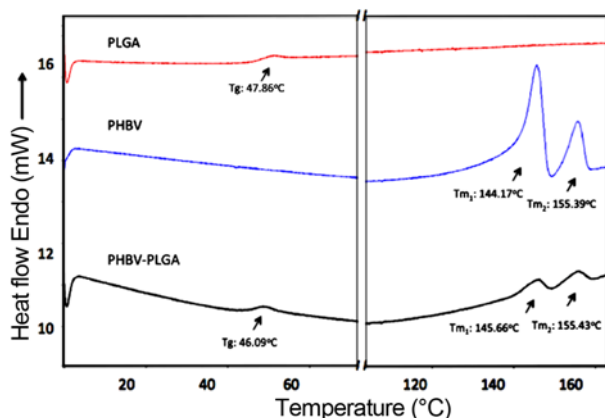


Figure 9. DSC thermograms of electrospun PLGA, PHBV, and PLGA/PHBV blend membrane.

blend membranes that can be determined by observation of the glass transition temperature of the blend [57].

Absorption of Wound Fluid

Absorption of excessive wound exudate is one of the most critical characteristics of an ideal wound dressing material. Thus, the absorption capacity of the lower layer of the bilayered wound dressing, which contacted the wound directly, was investigated and PLGA/PHBV membrane without CA and PLGA/PHBV film prepared by solvent casting method were used as controls. PECF was used as wound fluid, and the absorption values for the membranes were obtained as 437% and 420% for electrospun membranes with and without CA, respectively. Non-fibrous of PLGA/PHBV film revealed only 4% absorption, and this value was consistency with the literature [59]. According to the results, CA containing membrane had a better absorption capacity than electrospun PLGA/PHBV membrane indicating the better exudate absorption capacity.

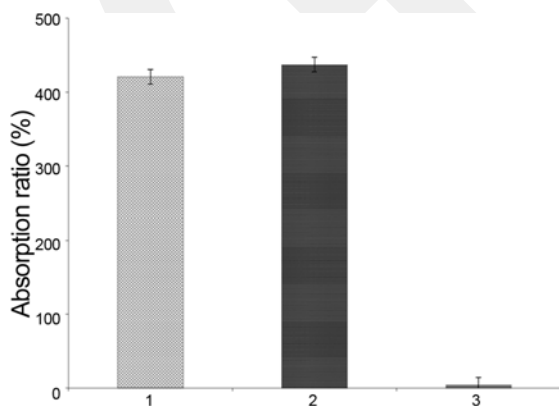


Figure 10. Absorption capacity of membranes; 1) electrospun PLGA/PHBV membrane, 2) electrospun PLGA/PHBV membrane with CA, and 3) non-fibrous film of PLGA/PHBV blend. Data points are the average of $n=3$, and error bars represent \pm SD.

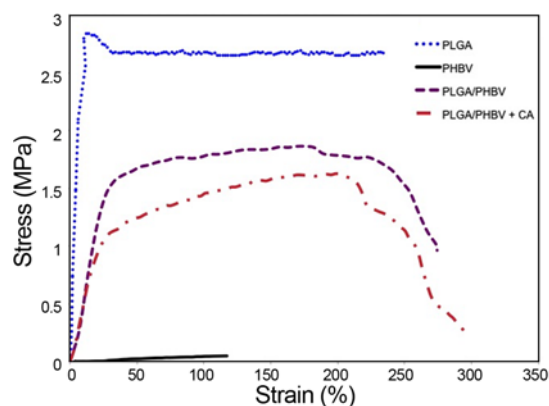


Figure 11. Typical stress-strain curves of electrospun PLGA, PHBV, PLGA/PHBV membranes with and without CA.

Mechanical Analysis

Typical stress-strain curves of neat PLGA, PHBV, and PLGA/PHBV electrospun membranes with and without CA at an initial strain rate of $1 \times 10^{-1} \text{ s}^{-1}$ are given in Figure 11. Our results indicate that the neat PLGA membrane showed the best strength value with plastic deformation and necking, while neat electrospun PHBV membrane showed the lowest strength and ductility values. Ultimate tensile strength values were found 1.86 MPa for PLGA/PHBV membrane without CA and 1.62 MPa for PLGA/PHBV membrane with CA, respectively. It can be seen that the electrospun PLGA/PHBV blend membrane with CA showed slightly lower strength values and ductility compared to the CA-free membrane. In our previous study working with the scientists from the mechanical engineering field, we investigated the specific mechanical behavior of the PLGA/PHBV and PHBV/PCL electrospun nonwoven mats with and without CA and demonstrated the effects of CA on the electrospun membranes' mechanical behavior at different strain rates [60]. According to the results, we observed that adding CA to the PLGA/PHBV electrospun membrane decreased the strength value with enhancing ductility slightly compared to the neat PLGA/PHBV at the different strain rates, as we also demonstrated in our recent study. The value for the ultimate tensile stress that we found in our recent study is 1.62 MPa, and it corresponds to 7.864 MPa as Young's Modulus. According to literature, the ultimate strength and Young's Modulus value indicated in our study is very similar to the values of the native skin tissue, whose Young's Modulus value is 4.6-20 MPa [61]. Thus, we can conclude that the mechanical property of the CA extract containing bilayered electrospun wound dressing designed in our study is adequate to be used for wound healing applications.

In vitro Release Profile of CA

In the literature, Gupta *et al.* showed that asiaticoside, an essential compound in CA, has a specific absorbance peak at

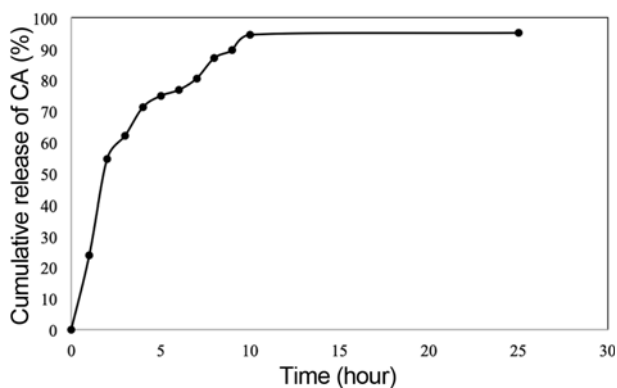


Figure 12. In vitro release profile of CA from electrospun PLGA/PHBV membrane.

215 nm [62]. Therefore, we monitored the amount of asiaticoside using the absorption peak at 215 nm for calculating the *in vitro* cumulative release of CA extract from electrospun PLGA/PHBV membrane. According to our result presented in Figure 12, the extract was rapidly released *in vitro* from the electrospun membrane in the first 5 hours, followed by a slow release over a prolonged period (24 h). Zhu *et al.* investigated the *in vitro* drug release profile of asiaticoside loaded electrospun alginate/PVA/chitosan membrane and showed that asiaticoside released from the membrane in 24 h [63]. Also, Suwantong *et al.* performed release study of asiaticoside from herb-loaded CA fiber mats, and they used two different types of release medium, which are 10 % methanol consisting of acetate buffer and PBS buffer. According to their result, asiaticoside release from the membrane in acetate medium and PBS medium reached plateau value at 720 and 480 minutes after immersion, respectively [64]. The *in vitro* release profile of CA from electrospun PLGA/PHBV membrane given herein is consistent well with previous studies. Based on the results, we conclude that the rapid release of CA from the membrane may be useful for the wound healing process.

Assessment of Cell Viability

MTS assay was conducted to evaluate the biocompatibility of electrospun membranes. Figure 13 presents the results. Membranes showed no significant differences in cytotoxicity at days of culture. Cell viability was calculated >95 % for all membranes, which approves that these membranes have not cytotoxic effect. Moreover, 1 % of CA content did not cause any toxicity to the membranes as well as poly(Q-4VP) in the applied dose. PLGA, PHBV, and poly(Q-4VP) are biocompatible and biodegradable polymers that have been widely investigated as wound dressing materials, as mentioned before.

Assessment of Cell Proliferation and Attachment

We tested the proliferation and attachment of human

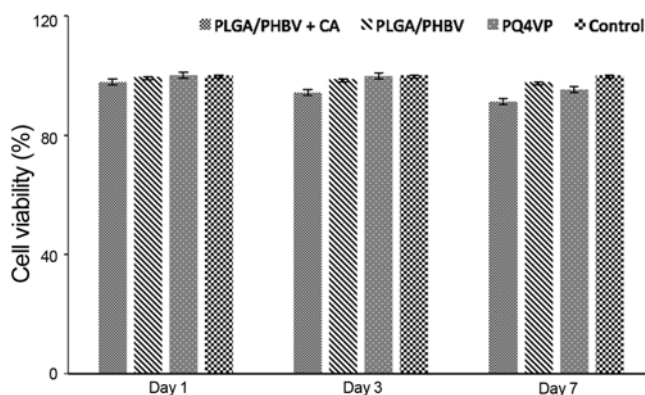


Figure 13. Viability (%) of human fibroblast cells on electrospun membranes following (A) 1 day or (B) 3 days and (C) 7 days of culture. Data points are the average of $n=3$, and error bars represent \pm SD.

fibroblast cells seeded on electrospun PLGA/PHBV membranes with and without CA by utilizing SEM on days 1, 4, and 7 (Figure 14). According to SEM images, fibroblasts adhered to both membranes and stretched across the fibrous substrates upon proliferation. As shown in Figure 13, the density of viable cells on both membranes was observed almost identical. Moreover, after seven days of cell culture, cell attachment on electrospun PLGA/PHBV membrane containing CA was better than that on neat electrospun PLGA/PHBV membrane. Previous studies reported that CA supports cell migration, proliferation, and growth [6,34,35]. Moreover, the appropriate surface morphology of fibers is one of the essential requirements for biocompatibility [2]. Thus, based on the SEM images, the surface and morphology of electrospun membranes are appropriate for skin reconstruction.

Conclusion

In our study, we successfully fabricated a novel antimicrobial bilayered wound dressing with a three-dimensional porous structure similar to that of the native ECM via electrospinning. The lower layer of the wound dressing, which directly contacted the wound, was designed from CA (1 %, w/v) containing electrospun PLGA/PHBV blend (75:25, w/w), while the upper layer was prepared from poly(Q-4VP) (60 %, w/v) by sequential and continuous electrospinning on the lower layer. Poly(4VP) was chemically modified to obtain quaternary form based on our previous study, in which antimicrobial characteristic of the poly(Q-4VP) was proved against the *E. coli* and *S. aureus*. Our results also demonstrated the significant effect of the lower layer of the wound dressing on the adhesion and proliferation of human fibroblast cells. Based on our results, the CA containing electrospun bilayered wound dressing fabricated and

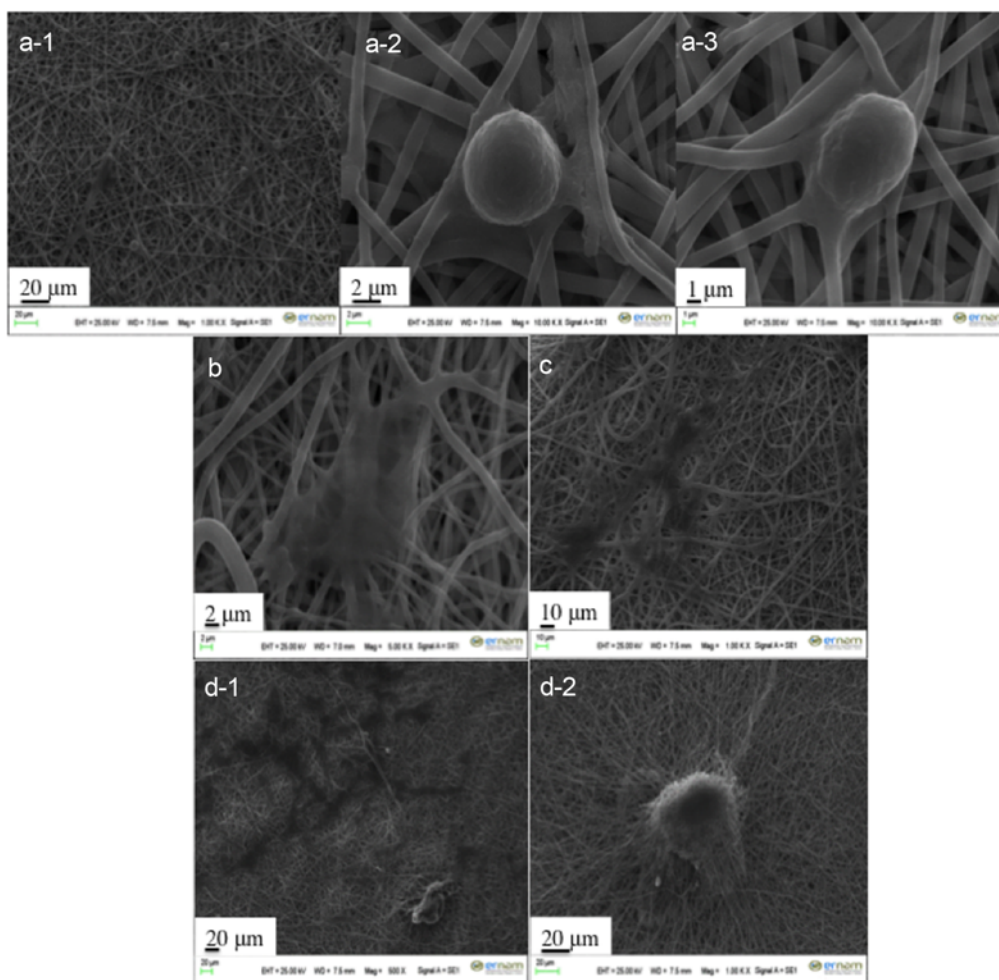


Figure 14. SEM images of the proliferation and attachment of human fibroblast cells; (a) on electrospun PLGA/PHBV membrane without CA, day 1, (b) day 4, (c) day 7, and (d) with CA, day 7.

characterized in this study could be an alternative to conventional wound care applications.

Acknowledgments

Authors acknowledge the financial support provided by Abdullah Gül University Scientific Research Projects under grant number FOA-2016-76.

References

1. S. Hosseinzadeh, M. Soleimani, M. Vossoughi, P. Ranjbarvan, S. Hamed, S. Zamanlui, and M. Mahmoudifard, *Mater. Sci. Eng. C.*, **75**, 653 (2017).
2. E. Zahedi, A. Esmaili, N. Eslahi, M. A. Shokrgozar, and A. Simchi, *Mar. Drugs.*, **17**, 27 (2019).
3. Z. Pedram Rad, J. Mokhtari, and M. Abbasi, *Iran. Polym. J. (English Ed.)*, **28**, 51 (2019).
4. C. H. Yao, C. Y. Lee, C. H. Huang, Y. S. Chen, and K. Y. Chen, *Mater. Sci. Eng. C.*, **79**, 533 (2017).
5. J. Wang and M. Windbergs, *Eur. J. Pharm. Biopharm.*, **119**, 283 (2017).
6. J. H. Lee, H. L. Kim, M. H. Lee, K. E. You, B. J. Kwon, H. J. Seo, and J. C. Park, *Phytomedicine*, **19**, 1223 (2012).
7. S. Tohidi, A. Ghaee, and J. Barzin, *Polym. Adv. Technol.*, **27**, 1020 (2016).
8. M. Norouzi, S. M. Boroujeni, N. Omidvarkordshouli, and M. Soleimani, *Adv. Healthc. Mater.*, **4**, 1114 (2015).
9. R. S. Tiğli Aydın, A. N. Eroğlu, A. Karakeçili, and A. Çalimli, *Fiber. Polym.*, **17**, 1765 (2016).
10. J. Wang, V. Planz, B. Vukosavljevic, and M. Windbergs, *Eur. J. Pharm. Biopharm.*, **129**, 175 (2018).
11. G. Jin, M. P. Prabhakaran, D. Kai, S. K. Annamalai, K. D. Arunachalam, and S. Ramakrishna, *Biomaterials*, **34**, 724 (2013).
12. A. Chanda, J. Adhikari, A. Ghosh, S. R. Chowdhury, S. Thomas, P. Datta, and P. Saha, *Int. J. Biol. Macromol.*, **116**, 774 (2018).

13. Y. F. Goh, I. Shakir, and R. Hussain, *J. Mater. Sci.*, **48**, 3027 (2013).
14. N. Charernsriwilaiwat, T. Rojanarata, T. Ngawhirunpat, M. Sukma, and P. Opanasopit, *Int. J. Pharm.*, **452**, 333 (2013).
15. E. Piskin, N. Bölgen, S. Egri, and I. A. Isoglu, *Nanomedicine*, **2**, 441 (2007).
16. S. J. Liu, Y. C. Kau, C. Y. Chou, J. K. Chen, R. C. Wu, and W. L. Yeh, *J. Memb. Sci.*, **355**, 53 (2010).
17. W. Zhao, J. Li, K. Jin, W. Liu, X. Qiu, and C. Li, *Mater. Sci. Eng. C.*, **59**, 1181 (2016).
18. E. Yüksel and A. Karakeçili, *Mater. Sci. Eng. C.*, **45**, 510 (2014).
19. P. Kuppan, S. Sethuraman, and U. M. Krishnan, *J. Biomater. Sci. Polym. Ed.*, **25**, 574 (2014).
20. G. Mutlu, S. Calamak, K. Ulubayram, and E. Guven, *J. Drug Deliv. Sci. Technol.*, **43**, 185 (2018).
21. S. Shahverdi, M. Hajimiri, M. A. Esfandiari, B. Larijani, F. Atyabi, A. Rajabiani, A. R. Dehpour, A. A. Gharehaghaji, and R. Dinarvand, *Int. J. Pharm.*, **473**, 345 (2014).
22. J. Varshosaz, A. Jahanian, and M. Maktoobian, *Fiber. Polym.*, **18**, 2125 (2017).
23. X. Liu, L. H. Nielsen, S. N. Klodzińska, H. M. Nielsen, H. Qu, L. P. Christensen, J. Rantanen, and M. Yang, *Eur. J. Pharm. Biopharm.*, **123**, 42 (2018).
24. L. Caihong, Z. Hailin, L. Jingjing, L. Jiuming, F. Xinxing, and C. Jianyong, *Polym. Eng. Sci.*, **55**, 907 (2015).
25. J. Yuan, J. Geng, Z. Xing, K.-J. Shim, I. Han, J.-C. Kim, I.-K. Kang, and J. Shen, *J. Tissue Eng. Regen. Med.*, **9**, 1027 (2015).
26. S. Y. H. Abdalkarim, H. Y. Yu, D. Wang, and J. Yao, *Cellulose*, **24**, 2925 (2017).
27. R. Ramalingam, C. Dhand, C. M. Leung, S. T. Ong, S. K. Annamalai, M. Kamruddin, N. K. Verma, S. Ramakrishna, R. Lakshminarayanan, and K. D. Arunachalam, *Mater. Sci. Eng. C.*, **98**, 503 (2019).
28. S. Suganya, S. Ram, B. S. Lakshmi, and V. R. Giridev, *J. Appl. Polym. Sci.*, **121**, 2893 (2011).
29. M. Ranjbar-Mohammadi and S. H. Bahrami, *Int. J. Biol. Macromol.*, **84**, 448 (2016).
30. B. Amri, E. Martino, F. Vitulo, F. Corana, L. B. Ben-Kaâb, M. Rui, D. Rossi, M. Mori, S. Rossi, and S. Collina, *Molecules*, **22**, 1851 (2017).
31. A. Saeidinia, F. Keihanian, F., A. P. Lashkari, H. G. Lahiji, M. Mobayyen, A. Heidarzade, and J. Golchai, *Medicine*, **96**, 61 (2017).
32. J. A. Ataide, L. C. Cefali, F. M. Croisfelt, A. A. Martins Shimojo, L. Oliveira-Nascimento, and P. V. Mazzola, *Phytother. Res.*, **32**, 1664 (2018).
33. J. Somboonwong, M. Kankaisre, B. Tantisira, and M. H. Tantisira, *BMC Comp. Alter. Med.*, **12**, 103 (2012).
34. O. Suwantong, U. Ruktanonchai, and P. Supaphol, *J. Biomed. Mater. Res.-Part A.*, **94**, 1216 (2010).
35. B. H. I. Ruszymah, S. R. Chowdhury, N. A. B. A. Manan, O. S. Fong, M. I. Adenan, and A. Bin Saim, *J. Ethnopharmacol.*, **140**, 333 (2012).
36. S. Kosalwatna, C. Shaipanich, and K. Bhanganada, *Siriraj Hosp. Gaz.*, **40**, 455 (1988).
37. A. Shukla, A. M. Rasik, G. K. Jain, R. Shankar, D. K. Kulshrestha, and B. N. Dhawan, *J. Ethnopharmacol.*, **65**, 1 (1999).
38. F. X. Maquart, F. Chastang, A. Simeon, P. Birembaut, P. Gillery, and Y. Wegrowski, *Eur. J. Dermatol.*, **9**, 289 (1999).
39. M. Liu, Y. Dai, Y. Li, Y. Luo, F. Huang, Z. Gong, and Q. Meng, *Planta Med.*, **74**, 809 (2008).
40. C.-Z. Zhang, J. Niu, Y.-S. Chong, Y.-F. Huang, Y. Chu, S.-Y. Xie, Z.-H. Jiang, and L.-H. Peng, *Eur. J. Pharm. Biopharm.*, **109**, 1 (2016).
41. P. Sikareepaisan, A. Suksamrarn, and P. Supaphol, *Nanotechnology*, **19**, 015102 (2008).
42. C.-H. Yao, J.-Y. Yeh, Y.-S. Chen, M.-H. Li, and C.-H. Huang, *J. Tissue Eng. Regen. Med.*, **11**, 905 (2017).
43. İ. A. İsoğlu, C. Demirkan, M. G. Şeker, K. Tuzlakoglu, and S. D. İsoğlu, *Fiber. Polym.*, **19**, 2229 (2018).
44. R. Qi, M. Shen, X. Cao, R. Guo, X. Tian, J. Yu, and X. Shi, *Analyst*, **136**, 2897 (2011).
45. M. Gong, C. Chi, J. Ye, M. Liao, W. Xie, C. Wu, R. Shi, and L. Zhang, *Coll. Sur. B: Biointerfaces*, **170**, 201 (2018).
46. F. Pourhojat, M. Sohrabi, S. Shariati, H. Mahdavi, and L. Asadpour, *Res. Chem. Intermed.*, **43**, 297 (2017).
47. A. Ehterami, M. Salehi, S. Farzamfar, A. Vaez, H. Samadian, H. Sahrapeyma, M. Mirzaii, S. Ghorbani, and A. Goodarzi, *Int. J. Biol. Macromol.*, **117**, 601 (2018).
48. Y. Yang, X. Zhu, W. Cui, X. Li, and Y. Jin, *Macromol. Mater. Eng.*, **294**, 611 (2009).
49. S. Manotham, K. Pengpat, S. Eitssayeam, G. Rujijanagul, D. R. Sweatman, and T. Tunkasiri, *Appl. Mech. Mater.*, **804**, 151 (2015).
50. W. Li, X. Yang, S. Feng, S. Yang, R. Zeng, and M. Tu, *J. Mater. Sci. Mater. Med.*, **29**, 117 (2018).
51. C. Fu, H. Bai, Q. Hu, T. Gao, and Y. Bai, *RSC Adv.*, **7**, 8886 (2017).
52. A. G. Vaishali, N. A. Rupali, and A. D. Sagar, *J. Chem. Pharm. Res.*, **8**, 122 (2016).
53. N. Geetha, K. Harini, Mary Joseph, R. Sangeetha, and P. Venkatachalam, *Iran J. Sci. Technol. Trans. Sci.*, **43**, 397 (2019).
54. P. Chowdhury, S. K. Saha, and S. P. Bayen, *J. Macromol. Sci. Part A Pure Appl. Chem.*, **50**, 976 (2013).
55. P. Mondal, S. K. Saha, and P. Chowdhury, *J. Appl. Polym. Sci.*, **127**, 5045 (2013).
56. C. Del Gaudio, E. Ercolani, F. Nanni, and A. Bianco, *Mater. Sci. Eng. A.*, **528**, 1764 (2011).
57. A. Wagner, V. Poursorkhabi, A. K. Mohanty, and M. Misra, *ACS Sustain. Chem. Eng.*, **2**, 1976 (2014).
58. F. Liu, R. Guo, M. Shen, S. Wang, and X. Shi, *Macromol. Mater. Eng.*, **294**, 666 (2009).
59. M. Liu, X. P. Duan, Y. M. Li, D. P. Yang, and Y. Z. Long, *Mater. Sci. Eng. C.*, **76**, 1413 (2017).

60. B. Bal, I. B. Tugluca, N. Koc, and I. A. Isoglu, *Mater. Res. Express*, **6**, 6 (2019).
61. R. S. Sequeira, S. P. Miguel, C. S. D. Cabral, A. F. Moreira, P. Ferreira, and I. J. Correia, *Pharmaceutics*, **570** (2019).
62. S. Gupta, P. Bhatt, and P. Chaturvedi, *World J. Microbiol. Biotechnol.*, **34**, 111 (2018).
63. L. Zhua, X. Liu, L. Du, and Y. Jin, *Biomed. Pharmacother.*, **83**, 33 (2016).
64. O. Suwantong, U. Ruktanonchai, and P. Supaphol, *Polymer*, **49**, 4239 (2008).

GCPRIS